Applied Nanoscience (2021) 11:2227–2234
https://doi.org/10.1007/s13204-021-01952-y

ORIGINAL ARTICLE

Green synthesis of magnetic α–Fe_2O_3 nanospheres using *Bridelia retusa* leaf extract for Fenton-like degradation of crystal violet dye

Raja Selvaraj[1] · Shraddha Pai[1] · Gokulakrishnan Murugesan[2] · Sadanand Pandey[3] · Ruchi Bhole[1] · Delicia Gonsalves[1] · Thivaharan Varadavenkatesan[4] · Ramesh Vinayagam[1]

Received: 23 April 2021 / Accepted: 18 June 2021 / Published online: 30 June 2021

Abstract

The reach of nanotechnology has permeated into a range of disciplines and systematically revolutionized many manufacturing techniques. Today, nanoparticles are fabricated using varied approaches, each with its pros and cons. Of them, the green synthesis approach has been very effective in terms of overall economics and the stability of nanoparticles. The current study investigates the use of the leaf extract of *Bridelia retusa* for the synthesis of iron oxide nanoparticles. Typical of these nanoparticles, no specific peak was discernible on employing UV–visible spectroscopy. The size, morphological features, and crystallinity of the nanoparticles were determined by employing scanning electron microscopy and electron diffraction spectroscopy. Almost uniformly sized at 38.58 nm, the nanoparticles were spherical, constituting elemental iron at 11.5% and elemental oxygen at 59%. Their relative composition confirmed the nanoparticles to be iron oxide. X-ray diffraction studies showed the particles to be hexagonal and rhombohedral, estimating the crystallite size at 24.27 nm. BET analysis put the pore volume at 0.1198 cm^3/g and pore diameter at 7.92 nm. The unique feature of the nanoparticles was that the specific surface area was 75.19 m^2/g, which is more than 12 times higher than commercial α-Fe_2O_3. The participation of a variety of biochemicals in the leaf extract towards the reduction-cum-stabilization was confirmed using FTIR analysis. The Fenton-like catalytic activity of the nanoparticles was put to test by attempting to degrade crystal violet dye, which was completely achieved in 270 min. The kinetics of the degradation was also modelled in the study.

Keywords Magnetic α-Fe_2O_3 nanoparticles · *Bridelia retusa* · Crystal violet dye · Fenton-like process · Green synthesis

Introduction

Nanoparticles are classified as objects with any one of their Cartesian dimensions to be within the range of 1–100 nm. Nanoparticles have managed to bridge the gap between macroscopic materials and atomic structures. They have a very high surface to volume ratio, due to which they have found a lot of use in medicinal and industrial processes. Nanotechnology is the engineering of substances at sub-atomic and sub-molecular scales. It involves the design, fabrication, characterization, and utilization of nanomaterials in potential areas. Nanotechnology saw its use in the late twentieth century and since then, has proved to be a great boon to science (Al-Hakkani et al. 2021).

Due to their ability to form a large variety of oxide compounds, metal oxides are used in many areas of physics, chemistry, and materials science (Rana et al. 2020). They can adapt to a large number of structural geometries and also showcase metallic, semiconductor, or insulator characteristics. They exhibit exquisite physical and chemical properties due to their high density and limited size. Iron oxide nanoparticles (IONs) have outstanding features such as good catalytic potential, adsorption capacity, biocompatibility, stability, and magnetic property (Rather and Sundarapandian

✉ Ramesh Vinayagam
ramesh.v@manipal.edu

1 Department of Chemical Engineering, Manipal Institute of Technology, Manipal Academy of Higher Education, Manipal, Karnataka 576104, India

2 Department of Biotechnology, M. S. Ramaiah Institute of Technology, Bengaluru, Karnataka 560054, India

3 Department of Chemistry, College of Natural Science, Yeungnam University, 280 Daehak-Ro, Gyeongsan 38541, Korea

4 Department of Biotechnology, Manipal Institute of Technology, Manipal Academy of Higher Education, Manipal, Karnataka 576104, India

2020). The magnetic property of the IONs makes them a straightforward choice for many processes since they can be easily removed from the mixture using a magnet at the end of the operation and can be reused. IONs come in various phases: FeO, gamma-Fe_2O_3, alpha-Fe_2O_3, Fe_3O_4 and alpha-FeO(OH). The last four forms are also known as maghemite, haematite, magnetite and goethite, respectively (Anchan et al. 2019; Golla-Schindler et al. 2006).

Many methods such as chemical, hydrothermal, solvothermal, and physical methods are available to synthesize IONs. Physical procedures are elaborate methods, which fail to control the size of the particles in the nanometer range. The major disadvantages are that they produce irregular-sized particles and the production cost is high (Vinayagam 2021). On the other hand, chemical methods involve the use of toxic solvents and hence, are not eco-friendly (Pai et al. 2021). Similarly, the hydrothermal and solvothermal methods are energy intensive. Therefore, the green synthesis of nanoparticles has gained much support as it utilizes non-toxic phytochemicals and also eliminates the hazardous substances which would have been encountered in chemical synthesis. It involves the use of bio-extracts as reducing agents, which in turn decreases the cost of the process to a large extent (Ali et al. 2016). Our research group has published a few IONs research articles using various plant extracts such as *Calliandra haematocephala* (Sirdeshpande et al. 2018), *Peltophorum pterocarpum* (Dash et al. 2019), *Spondias dulcis* (Vinayagam et al. 2020a), *Mussaenda erythrophylla* (Vinayagam 2021), *Thunbergia grandiflora* (Pai et al. 2021), and *Cynometra ramiflora* (Bishnoi et al. 2018).

Bridelia retusa tree belongs to the *Euphorbiaceae* family and can be recognized by its strong leather-like leaves and prominent spines on the bark of the stems. Many parts of the plant have been used for different purposes in traditional medicine (Kurdekar et al. 2013). On phytochemical analysis, it was found that the leaves, stem, and bark of *B. retusa* contain tannins, steroids, alkaloids, glucosides, and glycosides. These phytocompounds could be used for the synthesis of metallic nanoparticles. Our research group has already documented the use of *B. retusa* leaves for the synthesis of silver nanoparticles (Vinayagam et al. 2018). However, there are no reports on the formation of IONs using the leaf extract of *B. retusa*.

Crystal violet is a basic triarylmethane dye. It has a history of being used medicinally due to its antibacterial, antifungal, and anthelmintic properties but is now outdated due to modern medicine (Mittal et al. 2010). After being let out into the environment, it does not degrade for a lengthy period. It is known to be carcinogenic and toxic at high concentrations. It can also affect marine life negatively if it is released into a water source (Mani and Bharagava 2015). To remove crystal violet from wastewaters, a range of methods have been used including adsorption, precipitation, photocatalysis, and Fenton processes (Nandhini et al. 2019). However, most of them are cost-intensive and time-consuming. Hence, the advanced oxidation method, Fenton-like process is rapid and employs ION or Fe^0 particles as the iron source and hydrogen peroxide to generate hydroxyl radicals (Xue et al. 2009). Also, they are performed under neutral or non-acidic pH conditions, unlike the Fenton process that necessitates the use of low pH. The Fenton-like process also observed the absence of sludge formation after treating the wastewater (Wang et al. 2016).

Therefore, the objectives of this study are to (1) synthesize BR-Fe_2O_3NPs using leaf extract of *B. retusa*; (2) characterize synthesized BR-Fe_2O_3NPs; (3) evaluate the Fenton-like catalytic capability of the BR-Fe_2O_3NPs to remove crystal violet (CV) dye.

Materials and methods

Materials

Ferrous sulphate ($FeSO_4.7H_2O$) sodium hydroxide (NaOH) as well as hydrogen peroxide (H_2O_2) were procured from Merck (India). Crystal violet (CV) dye was obtained from Himedia, India. All the containers was suitably acid-cleaned and then cleaned with distilled water.

Preparation of *Bridelia retusa* leaf extract (BRLE)

The *B. retusa* leaves, collected on the Manipal Institute of Technology campus, were washed with tap water followed by distilled water washing to remove the dirt and surface-adherent materials. The air-dried leaves were made into small parts and boiled in 100 ml of distilled water at a ratio of 1:10. The resultant contents yielded a clear yellow filtrate after cooling which was preserved at 4 °C for further purposes (Vinayagam et al. 2018).

Formation of BR–Fe_2O_3NPs

0.1 M $FeSO_4.7H_2O$ solution and clear yellow BRLE were mixed in equal volume, with pH adjusted to 11 by the addition of 2 N NaOH. The solution turned to black from deep green upon boiling for 30 min at 90 °C in a thermostat which indicated the synthesis of BR-Fe_2O_3NPs.The formed NPs were separated using a powerful magnet and rinsed multiple times with distilled water. In the end, the product was oven-dried at 80 °C and stored in an air-tight container for further usage (Anchan et al. 2019).

Characterization of BR–Fe_2O_3NPs

The purified BR–Fe_2O_3NPs were analysed using several approaches. The morphological features of the BR–Fe_2O_3NPs was deduced by Field Emission Scanning Electron Microscope (FESEM) (Carl Zeiss), and Energy-dispersive X-ray Spectroscopy (EDX), respectively. X-ray diffractometer (XRD) (Miniflex 600, Rigaku) evaluated the crystallinity of BR-Fe_2O_3NPs. Pore volume as well as specific surface area (SSA) were ascertained using BET apparatus (Smart Instru). FTIR spectrophotometry (8400S Shimadzu) identified the functional groups in the NPs.

Catalysis for dye degradation

Experiments were conducted similar to the procedure opted in our earlier study (Anchan et al. 2019), with slight alterations in the quantities of the compounds. Typically, 10 mg of BR–Fe_2O_3NPs were added to a conical flask containing a solution of 3 mL CV dye and 300 µL H_2O_2. This flask was placed in a rotary shaker to be agitated for proper mixing at 150 rpm. Periodically, a specific volume was sampled out using a magnet to assure that no NPs were present in the sample. The absorbance spectrum of this sample was determined using the UV–visible spectrophotometer. A standard plot at 590 nm was used to ascertain the concentration of the dye. The kinetics of CV dye removal was modelled using first as well as second-order kinetic models (Shahwan 2011) given by Eqs. (1) and (2):

$$\ln\left[\frac{C_t - C_e}{C_0 - C_e}\right] = -k_1 t \tag{1}$$

$$\left[\frac{1}{C_t - C_e}\right] - \left[\frac{1}{C_0 - C_e}\right] = k_2 t \tag{2}$$

where C_0, C_t, C_e denote CV concentration to begin with, at time 't' and equilibrium, respectively. k_1 and k_2 are the first and second-order degradation rate constants, respectively.

Results and discussions

Visual observation and UV–vis studies

The synthesis process of BR–Fe_2O_3NPs was visually monitored. A light-ochre solution of BRLE [Fig. 1B] and pale yellow solution of $FeSO_4$ [Fig. 1C] were combined and the pH was then brought up to 11 by dropwise addition of 2 N NaOH solution. The prepared solution was then kept for heating at 90 °C for 30 min. A black-colored solution that was colloidal was obtained. This light brown to black color change confirmed the formation of IONs (Hoag et al. 2009). These were magnetic which can be observed in Fig. 1D.

UV–vis spectroscopy was performed on a multi-diluted solution of colloidal BR–Fe_2O_3NPs and the spectrum recorded was studied [Fig. 2]. The absence of any specific peak in the spectrum confirmed the formation of BR–Fe_2O_3NPs. This kind of spectrum is typical for BR–Fe_2O_3NPs which is in concordance with the studies performed by several researchers (Anchan et al. 2019; Vinayagam et al. 2020b).

It is known that the leaf extract of *B. retusa* contains a variety of phytocompounds (Mali and Borges 2003) and the standard reduction potential of them is sufficient to reduce

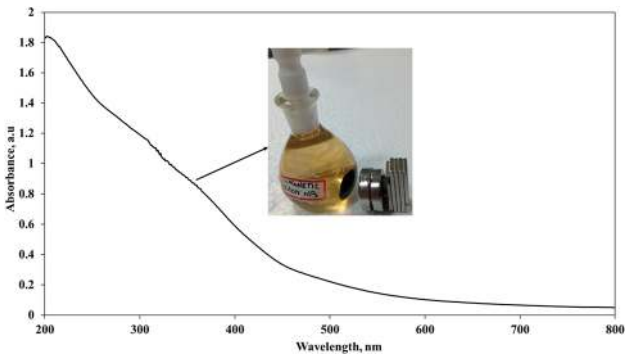

Fig. 2 UV–visible spectra of BR–Fe_2O_3NPs

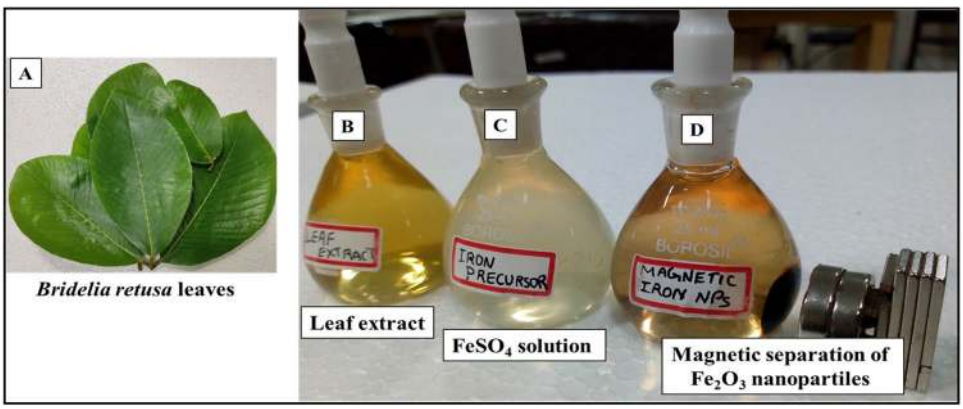

Fig. 1 Synthesis of BR–Fe_2O_3NPs

metallic elements to their respective nanoparticles as demonstrated in our earlier studies (Anchan et al. 2019; Groiss et al. 2017). Therefore, initially, Fe^{2+} ions were reduced to zero-valent iron particles by the phytocompounds of the leaf extract spontaneously. Since iron belongs to the first-row transition metal group and it has very high reactivity and is unstable. Therefore, the zero-valent iron particles were oxidized to form Fe^{3+} under basic conditions. In the end, aggregation followed by nucleation resulted in the formation of Fe2O3 nanoparticles which were capped by the phytocompounds. A similar kind of mechanism was already reported by our research group earlier for various IONs synthesized using plant extracts (Vinayagam 2021; Vinayagam et al. 2020a).

SEM–EDX

The BR–Fe_2O_3NPs, obtained through green synthesis, are shown in Fig. 3A. The surface morphology of these nanoparticles was studied using SEM image analysis. The average particle size was observed to be 38.58 nm using ImageJ software analysis. These particles were spherical and almost uniform in size. Similar kinds of nano-spherical magnetic nanoparticles were reported using various plant extracts in the literature and depicted in Table 1. Clusters of nanoparticles were probably due to the magnetic interactions between the nanoparticles.

EDX evaluated element-wise composition of a sample. From Fig. 3B it is clear that the prominent signals between 6 and 8 keV signify the presence of elemental Fe (Anchan et al. 2019) at 11.48%. The presence of elemental oxygen was confirmed due to the sharp peak at 0.5 keV at 59.02%. It can be seen in the EDX spectrum, that the oxygen peak is comparatively higher than the elemental iron peak. This confirms that the nanoparticles were of iron oxide. The presence of a minor peak at 0.3 keV signifies the presence of carbon (29.5%), originating from the biomolecules of the leaf extract (Vinayagam et al. 2020a). The purity of the nanoparticles is highlighted by the fact that no other peaks were witnessed in the spectrum.

XRD

The XRD spectrum of the synthesized BR-Fe_2O_3NPs is given in Fig. 4. The XRD spectra showed well-defined peak positions with 2θ values of 32.91 °, 35.41 °, 40.63 °, 49.21 °, 53.85 °, 62.25 °, and 63.77 ° which correspond to the phase planes of (104), (110), (113), (024), (116), (214), and (300). These values were in accordance with α-Fe_2O_3 nanoparticles obtained from JCPDS (File No. 33–0664) (Alagiri and Hamid 2014), thus corroborating the formation of a crystalline hexagonal rhombohedral structure. The average crystallite size of synthesized BR-Fe_2O_3NPs, as evaluated by the Debye–Scherrer equation was 24.27 nm. The lattice parameters were calculated as $a = 0.505$ nm and $c = 1.389$ nm. These results are consistent with our prior studies of green synthesized BR-Fe_2O_3NPs (Anchan et al. 2019; Vinayagam et al. 2020b). The absence of extra diffraction peaks indicates that

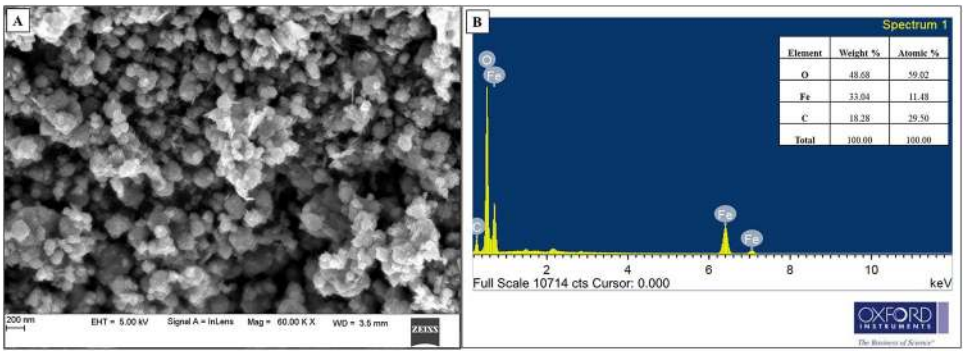

Fig. 3 FESEM and EDX of BR–Fe_2O_3NPs

Table 1 Size of spherical magnetic nanoparticles using few plant extracts

S. no	Plant source	Size of spherical IONs (nm)	Reference
1	*Juglans regia* green husk	5.7	Izadiyan (2020)
2	Green tea leaves	30–100	Lin et al. (2020)
3	*Couroupita guianensis* Aubl. Fruit	17	Sathishkumar et al. (2018)
4	*Teucrium polium* leaves	5.68–30.29	Kouhbanani et al. (2019)
5	*Lathyrus sativus* peel	NA	Dhar et al. (2021)
6	*Bridelia retusa* leaves	38.58	This study

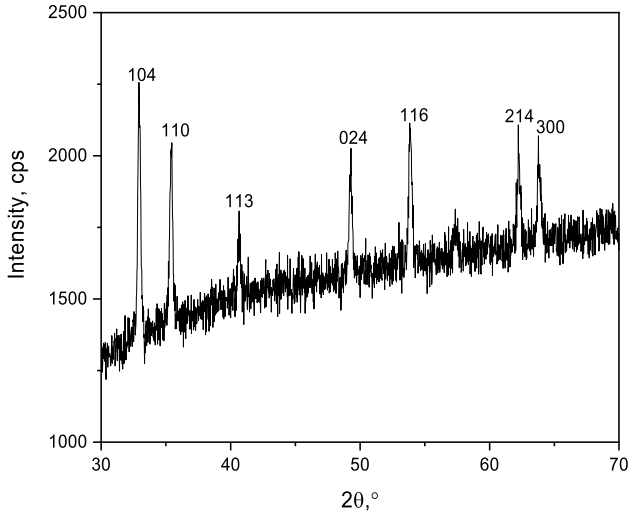

Fig. 4 XRD of BR–Fe_2O_3NPs

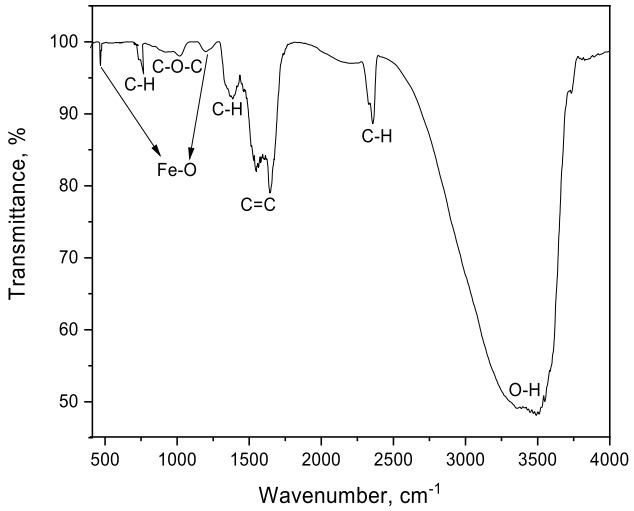

Fig. 5 FTIR spectrum of BR–Fe_2O_3NPs

the synthesized BR–Fe_2O_3NPs were of high purity as well as good crystallinity.

BET analysis

BET analysis performed on the synthesized BR–Fe_2O_3NPs attained SSA and pore volume of 75.19 m^2/g and 0.1198 cm^3/g, correspondingly. The SSA obtained in the present study is 12.5 times higher than that for commercial Fe_2O_3 (Ahmmad 2013) which indicated that the synthesized α-BR–Fe_2O_3NPs has a very porous structure. The large SSA may be due to the small average crystallite size observed during the X-ray diffraction studies. The pore diameter of the nanoparticles was found out to be 7.92 nm. Mesoporous particles have a pore diameter range of 2–50 nm. Hence, BR–Fe_2O_3NPs were concluded to be mesoporous. Owing to the large surface area and mesoporous structure, they act as excellent catalysts (Ali et al. 2018).

FTIR Analysis

Fourier-transform infrared spectroscopy (FTIR) is an analytical technique used to recognize the various functional groups existing in the synthesized nanoparticles (Hassan et al. 2020). It can be observed from Fig. 5 that the FTIR spectra of BR–Fe_2O_3NPs revealed strong bands at 3509, 2357, 1643, 1549, 1370, 1198, 1018, 469, and 768 (cm^{-1}). The wideband at 3509 cm^{-1} can be accredited to O–H stretching inside carboxylic acid or polyphenols, due to their presence in the BRLE. The band present at 2357 cm^{-1} can be recognized either as weak C≡C stretching in alkyne (Karpagavinayagam and Vedhi 2019), C–H stretching caused by aliphatic and aromatic compounds (Aksu Demirezen et al. 2019), or S–N vibrations of amino acids present in the BRLE. The bands at 1643 and 1549 cm^{-1} are because of the C = C bonds present in the BR-Fe_2O_3NPs. The band present at 1198 cm^{-1} is that of crystalline Fe–O vibrations (Sharma et al. 2020). This is a characteristic band for α-Fe_2O_3 nanoparticles thus corroborating the formation of hematite NPs (Kouhbanani et al. 2019). The 1018 cm^{-1} band indicates the aromatic stretching of the C–O–C bond (Yi et al. 2019). The 768 cm^{-1} band corresponds to C–H bending because of the presence of aromatic compounds (Yew 2016). The absorption band at 469 cm^{-1} is caused by vibrations due to Fe–O bond stretching (Raja et al. 2015). Similar bands were attained during our prior study of the synthesis of BR-Fe_2O_3NPs by using *S. dulcis* leaf extract (Vinayagam et al. 2020b). The presence of the functional groups in the FTIR spectrum corroborates the interaction between BRLE and the synthesized BR-Fe_2O_3NPs.

Catalysis for dye degradation

The degradation of CV dye by BR-Fe_2O_3NPs along with H_2O_2 is shown in Fig. 6. Vial A containing CV dye and H_2O_2 did not exhibit any substantial drop in the hue intensity. Vial B containing BR-Fe_2O_3NPs, CV dye, and H_2O_2 showed a significant transformation in the intensity of color. From the Linear plot of rate equation for CV dye degradation (Fig. 7), it is evident that it took approximately 270 min for the dye to completely degrade. The rapidity of the degradation process can be accredited to the Fe^{3+} of BR–Fe_2O_3NPs (Xue et al. 2009). Due to the magnetic property of the BR-Fe_2O_3NPs, they were removed using a magnet post the degradation of CV dye (Vial B). The complete attraction of nanoparticles to the magnet confirms the magnetic separation of CV dye using α-BRFe_2O_3NPs.

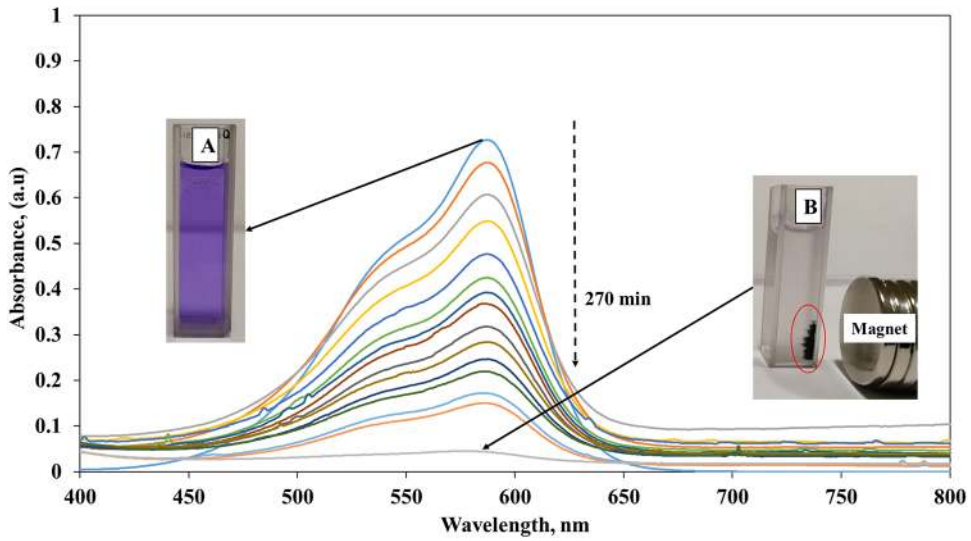

Fig. 6 Fenton-like catalysis of CV dye degradation by BR–Fe_2O_3NPs

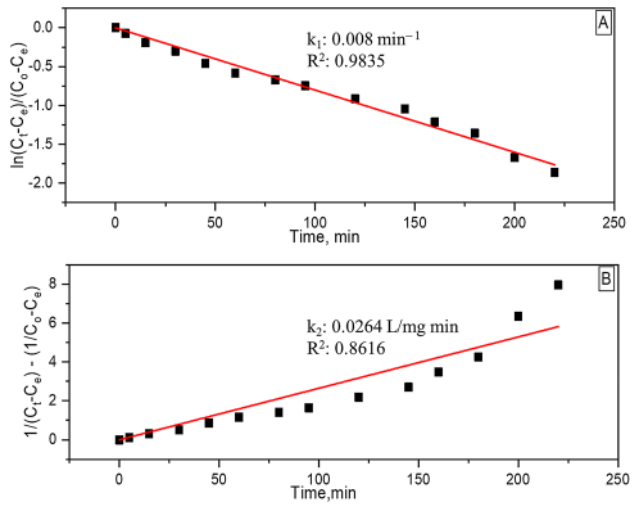

Fig. 7 Linear plot of first (**A**) and second-order (**B**) rate equation for CV dye degradation

During the degradation process, highly active hydroxyl radicals (HO·) are generated, as explained further. The Fe^{3+} of the BR-Fe_2O_3NPs establishes an intermediate by surface adsorption of H_2O_2. This intermediate split to form ferrous ion, hydrogen ion, and hydroperoxyl radical. The ferrous ion oxidizes to ferric ion along with the generation of a hydroxide ion and hydroxyl radical that play an important role in decolorization due to the strong oxidation capacity of H_2O_2. The generated hydroxyl radical reacts with CV dye to give colorless non-hazardous products. A similar mechanism was reported in the literature to degrade dye using Fenton-like green synthesized iron oxide nanoparticles (Anchan et al. 2019).

Linear plots were made to fit the degradation process using Eq. 1 and 2. These plots can be seen in Fig. 7. A first-order plot possessing good linearity was obtained (Fig. 7A). *R*-squared value was 0.9835 for first-order equation and 0.8616 for the second order. Degradation constants were calculated to be 0.008 min^{-1} (k_1) and 0.0264 L/mg.min (k_2). Thus it can be concluded that first-order kinetics is the most optimal fit for the decolorization process.

Conclusion

Herein, the leaf extract contents in *Bridelia retusa* were employed as a reductant to fabricate BR–Fe_2O_3NPs from $FeSO_4$, without using toxics or energy-intensive steps. The synthesized spherical BR–Fe_2O_3NPs characterized by XRD determined the presence of α-Fe_2O_3. The surface area obtained was 12.5 times higher than the commercial α-Fe_2O_3. FTIR results showed specific bands at 1198 cm^{-1} for Fe–O. The synthesized BR–Fe_2O_3NPs showed complete catalytic degradation of CV dye within 270 min by Fenton-like process. These findings pave a possible future path towards remediating dye-laden wastewater.

Acknowledgements The authors are grateful to the Department of Chemical Engineering, Manipal Institute of Technology, Manipal Academy of Higher Education for providing lab facilities and equipment to perform this study. The authors thank DST PURSE Laboratory, Mangalore University, Mangalagangotri for providing the FE–SEM and EDS facilities.

Funding Open access funding provided by Manipal Academy of Higher Education, Manipal.

Data availability The raw/processed data required to reproduce these findings cannot be shared at this time as the data also forms part of an ongoing study.

Declarations

Conflict of interest The authors declare that they have no conflict of interest.

References

Ahmmad B et al (2013) Green synthesis of mesoporous hematite (α-Fe2O3) nanoparticles and their photocatalytic activity. Adv Powder Technol 24(1):160–167. https://doi.org/10.1016/j.apt.2012.04.005

AksuDemirezen D, Yıldız YŞ, Yılmaz Ş, Demirezen Yılmaz D (2019) Green synthesis and characterization of iron oxide nanoparticles using *Ficus carica* (common fig) dried fruit extract. J Biosci. Bioeng 127(2):241–245. https://doi.org/10.1016/j.jbiosc.2018.07.024

Alagiri M, Hamid SBA (2014) Green synthesis of α-Fe2O3 nanoparticles for photocatalytic application. J Mater Sci Mater Electron 25(8):3572–3577. https://doi.org/10.1007/s10854-014-2058-0

Al-Hakkani MF, Gouda GA, Hassan SHA (2021) A review of green methods for phyto-fabrication of hematite (α-Fe2O3) nanoparticles and their characterization, properties, and applications. Heliyon 7(1):e05806. https://doi.org/10.1016/j.heliyon.2020.e05806

Ali A, Hira Zafar MZ, ulHaq I, Phull AR, Ali JS, Hussain A (2016) Synthesis, characterization, applications, and challenges of iron oxide nanoparticles. Nanotechnol Sci Appl 9:49–67

Ali I, Peng C, Ye T, Naz I (2018) Sorption of cationic malachite green dye on phytogenic magnetic nanoparticles functionalized by 3-marcaptopropanic acid. RSC Adv 8(16):8878–8897. https://doi.org/10.1039/C8RA00245B

Anchan S, Pai S, Sridevi H, Varadavenkatesan T, Vinayagam R, Selvaraj R (2019) Biogenic synthesis of ferric oxide nanoparticles using the leaf extract of Peltophorum pterocarpum and their catalytic dye degradation potential. Biocatal Agric Biotechnol 20:101251

Bishnoi S, Kumar A, Selvaraj R (2018) Facile synthesis of magnetic iron oxide nanoparticles using inedible *Cynometra ramiflora* fruit extract waste and their photocatalytic degradation of methylene blue dye. Mater Res Bull 97:121–127. https://doi.org/10.1016/j.materresbull.2017.08.040

Dash A, Ahmed MT, Selvaraj R (2019) Mesoporous magnetite nanoparticles synthesis using the Peltophorum pterocarpum pod extract, their antibacterial efficacy against pathogens and ability to remove a pollutant dye. J Mol Struct 1178:268–273

Dhar PK, Saha P, Hasan MK, Amin MK, Haque MR (2021) Green synthesis of magnetite nanoparticles using Lathyrus sativus peel extract and evaluation of their catalytic activity. Clean Eng Technol 3:100117. https://doi.org/10.1016/j.clet.2021.100117

Golla-Schindler U, Hinrichs R, Bomati-Miguel O, Putnis A (2006) Determination of the oxidation state for iron oxide minerals by energy-filtering TEM. Micron 37(5):473–477. https://doi.org/10.1016/j.micron.2005.11.002

Groiss S, Selvaraj R, Varadavenkatesan T, Vinayagam R (2017) Structural characterization, antibacterial and catalytic effect of iron oxide nanoparticles synthesised using the leaf extract of Cynometra ramiflora. J Mol Struct 1128:572–578. https://doi.org/10.1016/j.molstruc.2016.09.031

Hassan W, Noureen S, Mustaqeem M, Saleh TA, Zafar S (2020) Efficient adsorbent derived from Haloxylon recurvum plant for the adsorption of acid brown dye: Kinetics, isotherm and thermodynamic optimization. Surfaces and Interfaces 20:100510. https://doi.org/10.1016/j.surfin.2020.100510

Hoag GE, Collins JB, Holcomb JL, Hoag JR, Nadagouda MN, Varma RS (2009) Degradation of bromothymol blue by 'greener' nano-scale zero-valent iron synthesized using tea polyphenols. J Mater Chem 19(45):8671. https://doi.org/10.1039/b909148c

Izadiyan Z et al (2020) Cytotoxicity assay of plant-mediated synthesized iron oxide nanoparticles using Juglans regia green husk extract. Arab J Chem 13(1):2011–2023. https://doi.org/10.1016/j.arabjc.2018.02.019

Karpagavinayagam P, Vedhi C (2019) Green synthesis of iron oxide nanoparticles using Avicennia marina flower extract. Vacuum 160:286–292. https://doi.org/10.1016/j.vacuum.2018.11.043

Kouhbanani MAJ, Beheshtkhoo N, Taghizadeh S, Amani AM, Alimardani V (2019) One-step green synthesis and characterization of iron oxide nanoparticles using aqueous leaf extract of Teucrium polium and their catalytic application in dye degradation. Adv Nat Sci Nanosci Nanotechnol 10(1):15007

Kurdekar R, Hegde G, Hebbar S (2013) Antimicrobial efficacy of *Bridelia retusa* (L.) Spreng and Asclepias curassavica L. Indian J Nat Prod Resour 3:589–593

Lin Z, Weng X, Owens G, Chen Z (2020) Simultaneous removal of Pb (II) and rifampicin from wastewater by iron nanoparticles synthesized by a tea extract. J Clean Prod 242:118476. https://doi.org/10.1016/j.jclepro.2019.118476

Mali S, Borges RM (2003) Phenolics, fibre, alkaloids, saponins, and cyanogenic glycosides in a seasonal cloud forest in India. Biochem Syst Ecol 31(11):1221–1246. https://doi.org/10.1016/S0305-1978(03)00079-6

Mani S, Bharagava R (2015) Exposure to crystal violet, its toxic, genotoxic and carcinogenic effects on environment and its degradation and detoxification for environmental safety. Rev Environ Contam Toxicol 237:71–104. https://doi.org/10.1007/978-3-319-23573-8_4

Mittal A, Mittal J, Malviya A, Kaur D, Gupta VK (2010) Adsorption of hazardous dye crystal violet from wastewater by waste materials. J Colloid Interface Sci 343(2):463–473. https://doi.org/10.1016/j.jcis.2009.11.060

Nandhini NT, Rajeshkumar S, Mythili S (2019) The possible mechanism of eco-friendly synthesized nanoparticles on hazardous dyes degradation. Biocatal Agric Biotechnol 19:101138. https://doi.org/10.1016/j.bcab.2019.101138

Pai S, Kini SM, Narasimhan MK, Pugazhendhi A, Selvaraj R (2021) Structural characterization and adsorptive ability of green synthesized Fe3O4 nanoparticles to remove Acid blue 113 dye. Surfaces and Interfaces 23:100947. https://doi.org/10.1016/j.surfin.2021.100947

Raja S, Ramesh V, Thivaharan V (2015) Antibacterial and anticoagulant activity of silver nanoparticles synthesised from a novel source–pods of Peltophorum pterocarpum. J Ind Eng Chem 29:257–264. https://doi.org/10.1016/j.jiec.2015.03.033

Rana A, Yadav K, Jagadevan S (2020) A comprehensive review on green synthesis of nature-inspired metal nanoparticles: Mechanism, application and toxicity. J Clean Prod 272:122880. https://doi.org/10.1016/j.jclepro.2020.122880

Rather MY, Sundarapandian S (2020) Magnetic iron oxide nanorod synthesis by *Wedelia urticifolia* (Blume) DC. leaf extract for methylene blue dye degradation. Appl Nanosci. https://doi.org/10.1007/s13204-020-01366-2

Sathishkumar G et al (2018) Green synthesis of magnetic Fe3O4 nanoparticles using Couroupita guianensis Aubl. fruit extract for their antibacterial and cytotoxicity activities. Artif Cells Nanomed Biotechnol 46(3):589–598. https://doi.org/10.1080/21691401.2017.1332635

Shahwan T et al (2011) Green synthesis of iron nanoparticles and their application as a Fenton-like catalyst for the degradation of aqueous cationic and anionic dyes. Chem Eng J 172(1):258–266. https://doi.org/10.1016/j.cej.2011.05.103

Sharma D, Ledwani L, Mehrotra T, Kumar N, Pervaiz N, Kumar R (2020) Biosynthesis of hematite nanoparticles using Rheum emodi and their antimicrobial and anticancerous effects in vitro. J Photochem Photobiol B Biol. https://doi.org/10.1016/j.jphotobiol.2020.111841

Sirdeshpande KD, Sridhar A, Cholkar KM, Selvaraj R (2018) Structural characterization of mesoporous magnetite nanoparticles synthesized using the leaf extract of Calliandra haematocephala and their photocatalytic degradation of malachite green dye. Appl Nanosci 8(4):675–683. https://doi.org/10.1007/s13204-018-0698-8

Vinayagam R, Varadavenkatesan T, Selvaraj R (2018) Green synthesis, structural characterization, and catalytic activity of silver nanoparticles stabilized with Bridelia retusa leaf extract. Green Process Synth 7(1):30–37. https://doi.org/10.1515/gps-2016-0236

Vinayagam R, Pai S, Varadavenkatesan T, Kumar M, Narayanasamy S, Selvaraj R (2020a) Structural characterization of green synthesized α-Fe2O3 nanoparticles using the leaf extract of Spondias dulcis. Surfaces Interfaces 20:100618. https://doi.org/10.1016/j.surfin.2020.100618

Vinayagam R, Pai S, Varadavenkatesan T (2020b) Structural characterization of green synthesized α -Fe 2 O 3 nanoparticles using the leaf extract of *Spondias dulcis*. Surfaces Interfac 20:1–9. https://doi.org/10.1016/j.surfin.2020.100618

Vinayagam R et al (2021) Structural characterization of green synthesized magnetic mesoporous Fe3O4NPs@ME. Mater Chem Phys 262:124323. https://doi.org/10.1016/j.matchemphys.2021.124323

Wang N, Zheng T, Zhang G, Wang P (2016) A review on Fenton-like processes for organic wastewater treatment. J Environ Chem Eng 4(1):762–787. https://doi.org/10.1016/j.jece.2015.12.016

Xue X, Hanna K, Deng N (2009) Fenton-like oxidation of Rhodamine B in the presence of two types of iron (II, III) oxide. J Hazard Mater 166(1):407–414. https://doi.org/10.1016/j.jhazmat.2008.11.089

Yew YP et al (2016) Green synthesis of magnetite (Fe3O4) nanoparticles using seaweed (*Kappaphycus alvarezii*) Extract. Nanoscale Res Lett 11(1):276. https://doi.org/10.1186/s11671-016-1498-2

Yi Y, Tu G, Tsang PE, Xiao S, Fang Z (2019) Green synthesis of iron-based nanoparticles from extracts of Nephrolepis auriculata and applications for Cr(VI) removal. Mater Lett 234:388–391. https://doi.org/10.1016/j.matlet.2018.09.137